# Correlation between valence electronic structure and magnetic properties in $R\mathrm{Co}_5$ ($R$ = rare earth) intermetallic compound*

Zhi-Qin Xue(薛智琴) and Yong-Quan Guo(郭永权)†

*North China Electric Power University, School of Energy Power and Mechanical Engineering, Beijing* 102206, *China*

(Received 26 October 2015; revised manuscript received 3 March 2016; published online 20 April 2016)

The magnetisms of $R\mathrm{Co}_5$ ($R$ = rare earth) intermetallics are systematically studied with the empirical electron theory of solids and molecules (EET). The theoretical moments and Curie temperatures agree well with experimental ones. The calculated results show strong correlations between the valence electronic structure and the magnetic properties in $R\mathrm{Co}_5$ intermetallic compounds. The moments of $R\mathrm{Co}_5$ intermetallics originate mainly from the 3d electrons of Co atoms and 4f electrons of rare earth, and the s electrons also affect the magnetic moments by the hybridization of d and s electrons. It is found that moment of Co atom at 2$c$ site is higher than that at 3$g$ site due to the fact that the bonding effect between R and Co is associated with an electron transformation from 3d electrons into covalence electrons. In the heavy rare-earth-based $R\mathrm{Co}_5$ intermetallics, the contribution to magnetic moment originates from the 3d and 4f electrons. The covalence electrons and lattice electrons also affect the Curie temperature, which is proportional to the average moment along the various bonds.

**Keywords:** EET theory, electronic structure, Curie temperature, $R\mathrm{Co}_5$ intermetallics

**PACS:** 31.10.+z, 31.30.–i **DOI:** 10.1088/1674-1056/25/6/063101

## 1. Introduction

Owing to the large magnetocrystalline anisotropies, high Curie temperatures and high saturation moments at room temperature, $R\mathrm{Co}_5$ ($R$ = rare earth) intermetallic compounds have received considerable scientific and technological attention in the past decades,[1,2] and the studies have covered the experiment, theory and technology for developing the advanced rare earth permanent magnetic materials.[3–5] The study on magnetic properties of $R\mathrm{Co}_5$ intermetallic compounds is derived from the magnetization measurements on single crystals.[6] Rao and Greedan have established the relationships between the basic parameters in crystal-field theory and the magnetocrystalline anisotropy in most $R\mathrm{Co}_5$ intermetallic compounds.[7] The single-ion anisotropy has been found to have a fundamental influence on the behavior of the magnetic system and the related mechanism has been studied.[8,9] In many cases, the single-ion anisotropy model contains many calculating parameters especially in the Heisenberg model proposed based on the exchange coupling interaction. As for the first principle theory, the magnetic properties of $R\mathrm{Co}_5$ compounds are usually discussed within a two-sublattice model consisting of R and Co sublattices.[10,11] The computational methods based on the density functional theory (DFT) provide an important insight into the electronic structure and the related physical properties for the various materials. The basic DFT approximation (local spin density approximation-LSDA) is usually restricted to the so-called open core treatment of the 4f electrons.[12,13] However, LSDA could not predict the energetics of the various magnetic orders due to the absence of the energy gap between the filled and the empty states and underestimations of the orbital magnetic moments.[14,15] The theoretical work on the anisotropy and Curie temperature of $R$–(Fe,Co) magnetic alloys were carried out in the molecular-field approximation by studying the exchange coupling interactions between the 3d electrons of Fe or Co and 4f electrons of rare earth.[16] However, there are too many theoretical parameters in the complicated calculation. Also, the samples should be of the single-crystal.[17]

As for the first principle theory, it could not initially be used to study the magnetism of rare-earth-based intermetallic compounds. In recent years, a framework of the LSDA + U approach has been developed to calculate the magnetic properties of rare earth alloys and compounds based on the mean-field theory.[18] However, the calculation is restricted by the structural cell model and the capacity of the computer. In the present paper, we use the empirical electron theory of solids and molecules (EET), which is based on Pauling's electron theory of metals.[19] Owing to its lesser computing parameters than the molecular-field and the first principle theories, the model is simpler than the theories of crystal-field and first-principle without considering any integral or differential calculation. The EET can be used to investigate the correlations between the valence electronic structures and multiple physical properties of solid state materials. The approximations, which are based on the electronic structures, can work in studying the essential mechanisms of physical phenomena as reported. On one hand, the electronic structure analyses could reveal many natures of physical phenomena such as: orbital hybridization, band gap between the highest oc-

*Project supported by the National Natural Science Foundation of China (Grant No. 11274110).

†Corresponding author. E-mail: yqguo@ncepu.edu.cn

© 2016 Chinese Physical Society and IOP Publishing Ltd 

cupied molecular orbital (HOMO) and the lowest unoccupied molecular orbital (LUMO), vertical ionization potentials, and electron affinities, which are important for studying the correlations between the electronic structures and physical properties in molecules and solids.[20–22] The multiple properties such as cohesive energy, melting point, transition temperature, magnetic moment, Curie temperature, superconductor temperature, etc. have been calculated based on the electron states in the electronic structure.[23–26] In this study, the magnetic moments and Curie temperatures of $R\mathrm{Co}_5$ ($R$ = Y, La, Ce, Pr, Nd, Sm, Gd, Tb, Dy, Er) intermetallics are systematically studied with EET and the relations between the electronic structures and magnetic characteristics of these compounds are discussed as well.

## 2. Empirical electron theory (EET)

EET is a semi-empirical theory based on the Pauling valence-bonding theory and Hume–Rothery electron concentration rule. As a supplement, the equivalence valence electron hypothesis is introduced for the application of the electron theory to the crystal structures. The theory consists of three general hypotheses and one method of calculating bond distances. Hypothesis 1: the atoms in a solid and a molecule are in general hybridization of the two states, which can be called the h (head) and t (tail) states. Both states have one or two kinds of valence electrons; that is, covalent and newly introduced lattice electrons. Hypothesis 2: the hybridization of the two states is discontinuous, allowing only certain relative compositions to be calculated by a $k$-equation. Hypothesis 3: the covalent bond length between atom $u$ and $v$ with the number of covalent electron pairs denoted by $n_\alpha$ is related by

$$\bar{D}_{uv}(n_\alpha) = R_u(l) + R_v(l) - \beta \log n_\alpha, \tag{1}$$

where $R_u(1)$ and $R_v(1)$ denote the radii of single-bond for u and v atoms, respectively. The parameter $\beta$ can reflect how much the electron clouds of the u and v atoms overlap each other, and $\beta$ values are 0.6 for metals and alloys and 0.71 for the other nonmetal compounds, respectively. Here a modification of Pauling's theory is made for $(n-1)$ value according to the maximum of $n_\alpha$ $(\alpha = A,B,C,\ldots,N)$, and the $(n-1)$ values are listed below.

$$\beta = \begin{cases} 0.6 \ \text{when the maximum} \ n_\alpha \in [0.2, 0.70], \\ 0.71 \ \text{when the maximum} \ n_\alpha \\ \text{is less than 0.25 or more than 0.75}, \\ 0.71 - 2.2\varepsilon \ \text{where} \ \ \varepsilon \in [0, 0.05], \\ \text{the maximum} \ n_\alpha = 0.25 + \varepsilon \text{or} 0.71 - \varepsilon. \end{cases} \tag{2}$$

The bond length difference (BLD) analytical method: the method is trying to find the derivations ($\Delta D$) between the theoretical $\overline{D}(n_\alpha)$ and experimental bond lengths $D(n_\alpha)$ until $\Delta D \leq 0.05$ Å. For calculating the theoretical bond lengths $\bar{D}(n_\alpha)(\alpha = A,B,C,\ldots N)$, the $n_\alpha(\alpha = A,B,C,\ldots,N)$ values should be first calculated based on $(\alpha = B,C,\ldots,N)$ experimental bond length difference $[D(n_A) - D(n_\alpha)]$ equations as reported in Ref. [17]. The theoretical bond lengths $D(n_\alpha)$ could be calculated by substituting the $n_\alpha$ $(\alpha = A,B,C,\ldots,N)$ values into Eq. (1).

From the derivation, it is seen that

$$\begin{aligned} \Delta D &= \bar{D}(n_A) - D(n_A) = \bar{D}(n_B) - D(n_B) \\ &= \bar{D}(n_C) - D(n_C). \end{aligned} \tag{3}$$

Hence the difference $\Delta D$ is a criterion for all the $\bar{D}(n_\alpha)$'s, that is, the theoretical explanation for all the $\bar{D}(n_\alpha)$'s of a crystalline or molecular structure. If it is smaller than 0.05 Å, it proves that the valence bond electron distribution is correct in the first order approximation. However, the only criterion limitation of $\Delta D$ is not enough to determine the electronic structure. Thus, the extra physical property criterions, such as melting point, cohesive energy, magnetic moments are necessary. Here the moment and Curie temperature criterions are discussed.

## 3. Calculations of magnetic moment and Curie temperature

### 3.1. Magnetic moments[23]

According to the criterion of $\Delta D \leq 0.05$ in the BLD method, the hybridization states of the electrons in solid and molecules could be determined, and the relative values of $C_{h\sigma}$ and $C_{t\sigma}$ are determined.

Then there is given the equation for calculating the magnetic moments:

$$m^{3\mathrm{d}} = C_{h\sigma} m_h^{3\mathrm{d}} + C_{t\sigma} m_t^{3\mathrm{d}}. \tag{4}$$

For a molecule, we then have

$$m^{3\mathrm{d}} = \sum_i^N m_i^{3\mathrm{d}} A_i, \tag{5}$$

where $A_i$ and $m_i^{3\mathrm{d}}$ denote the atom number of the $i$-th atom and its 3d magnetic electron number. The $\Delta m$ is also considered as a criterion for all the $m^{3\mathrm{d}}$ for the Co atoms at $2c$ and $3g$ sites, and expressed as

$$\Delta m = \overline{m_{R\mathrm{Co}_5}}(n_\alpha) - m_{\mathrm{Co}_5}(n_\alpha), \tag{6}$$

with

$$\overline{m_{\mathrm{Co}_5}} = \left| 2m_{2c}^{3\mathrm{d}} + 3m_{3g}^{3\mathrm{d}} \pm m_R^{\mathrm{obs}} \right|, \tag{7}$$

where the $\overline{m_{\mathrm{Co}_5}}(n_\alpha)$ and $m_{\mathrm{Co}_5}(n_\alpha)$ are corresponding to the theoretical and observed magnetic moments.

The magnetic moments of rare earth $m_R^{\mathrm{obs}}$ are the theoretical moments in ordered status $g\mu_{\mathrm{B}}J$ ($J$ is angular momentum). The moment contributed by 4f electron of rare earth depends on 4f electron spin alignment at $R$ sublattice, and its values are positive for light rare-earth- (LRE) based $R\mathrm{Co}_5$ compounds and negative for the heavy rare-earth- (HRE) based

$R$Co$_5$ compounds, respectively. Therefore, the average magnetic moment per atom is

$$\bar{m}/\text{atom} = \frac{\overline{m_{\text{Co}_5}}}{\sum_{i=1}^{N} A_i}. \tag{8}$$

About all, the criterion $\Delta m$ gives another limitation for estimating the calculations.

### 3.2. Curie temperature

The model for calculating Curie temperature is based on the assumption of molten ferromagnetic order structure by the heat vibrations induced by the phonon energy with increasing temperature. When the temperature reaches a certain value of $T_c$, the phonon energy equals the magnetic energy. If $T > T_c$, the magnetic order is molten and the ferromagnetic characteristics disappear. This transition temperature is regarded as the Curie temperature. The energy of $N$ phonons is

$$U_P = \frac{3}{2}NkT.$$

The average magnetic energy per bond is

$$U_m = g\frac{a\overline{\text{m}_{\text{Co}_5}}}{\sum_{\alpha=A}^{N} I_\alpha \gamma_\alpha} \quad (\alpha = A, B, \ldots, N), \tag{9}$$

where $U_\text{p}$ and $U_\text{m}$ denote the phonon and magnetic energy, respectively. When $U_\text{p} = U_\text{m}$, and $g = 2.2$ for Co, then we have

$$T_\text{c} = \frac{C}{3R}\frac{g\overline{m_{\text{Co}_5}}}{\sum_{\alpha=A}^{N} I_\alpha \gamma_\alpha}, \tag{10}$$

where $R = 8.31$ J/mol, and $C = 1.542 \times 10^4$.

Then here is given the criterion, $\Delta T_\text{c}$.

$$\Delta T_\text{c} = \overline{T_\text{c}} - T_\text{c}, \tag{11}$$

where the $\overline{T_\text{c}}$ and $T_\text{c}$ denote the calculated and observed Curie temperature respectively.

In summary, the theoretical $\overline{D}(n_\alpha)$'s should fit to all the limitations of $\Delta D$, $\Delta m$, and $\Delta T_\text{c}$ well, and then the relations between the magnetic characteristics and electronic structures in the exact hybridization can be revealed. The calculated results are listed in Tables 1–3.

## 4. Calculated results and discussion

### 4.1. Crystal structures of $R$Co$_5$ compounds

$R$Co$_5$ compounds crystallize into the hexagonal CaCu$_5$-type structure with a space group of $P6/mmm$, and the atomic occupations are $1a$ for $R$, $2c$ for Co$^\text{I}$, $3g$ for Co$^\text{II}$, respectively. The lattice parameters of $R$Co$_5$ compounds and the valence bond lengths of $R$–Co and Co–Co bonds are listed in Table 1. Based on EET, the shortest atomic bond will seriously hamper the magnetization direction, whose density of covalent electron pairs $(n_\alpha)$ is the largest. In Table 1, the valence bond length of Co$^\text{I}$–Co$^\text{II}$ is the shortest, which indicates the interactions between Co$^\text{I}$–Co$^\text{II}$ is the strongest, and $R$–Co$^\text{I}$ is the second strongest, respectively. As previously reported,[9] the $R$–$R$ exchange interaction, which is much weaker than that of $R$–Co, could be ignored in this calculation. The atomic radii of rare earth elements except for Y element decrease gradually with increasing the atomic number of rare earth element,[27] which causes the lattice parameters and the valence bond lengths to decrease. The shorter the valence bond length is, the stronger the cohesive energy between the bonded atoms is. As for the abnormal decreases of those parameters in CeCo$_5$ compound, the cohesive energy might be affected by the mixed valence of Ce-ion (+3, +4).

**Table 1.** Lattice parameters of $R$Co$_5$ and valence bond lengths.

| $R$Co$_5$ | YCo$_5$ | LaCo$_5$ | CeCo$_5$ | PrCo$_5$ | NdCo$_5$ | SmCo$_5$ | GdCo$_5$ | TbCo$_5$ | DyCo$_5$ | ErCo$_5$ |
|---|---|---|---|---|---|---|---|---|---|---|
| $a$/Å | 4.951 | 5.120 | 4.920 | 5.012 | 5.010 | 5.002 | 4.975 | 4.961 | 4.924 | 4.885 |
| $c$/Å | 3.975 | 3.980 | 4.029 | 3.990 | 3.960 | 3.964 | 3.974 | 3.981 | 3.986 | 4.002 |
| $R$–Co$^\text{I}$/Å | 2.859 | 2.956 | 2.840 | 2.894 | 2.893 | 2.888 | 2.872 | 2.864 | 2.843 | 2.820 |
| $R$–Co$^\text{II}$/Å | 3.175 | 3.242 | 3.179 | 3.203 | 3.193 | 3.191 | 3.183 | 3.180 | 3.168 | 3.158 |
| Co$^\text{I}$–Co$^\text{II}$/Å | 2.448 | 2.479 | 2.465 | 2.465 | 2.452 | 2.452 | 2.451 | 2.452 | 2.448 | 2.448 |

### 4.2. Calculation of magnetic moment and Curie temperature

The calculated results of magnetic properties are given in Table 2. As shown in Figs. 1 and 2, the calculated results are in good agreement with the experimental results. It reveals that the magnetic moment of Co$^\text{I}$ is larger than that of Co$^\text{II}$, which is consistent with the result of neutron diffraction experiment.[28] The moment of Co$^\text{II}$ at $3g$ is weakened due to the exchange coupling interaction between Co$^\text{II}$ at $3g$ and $R$ at $1a$ site. According to Fig. 1, it can be found that the moments of $R$Co$_5$ are strongly related to those of rare earths. The change tendency of $R$Co$_5$ ($R$ is light rare earth) is similar to that of $R$. However, in the heavy rare earth regime, the two moment curves seem to be axisymmetric due to the negative moment of the heavy rare earth. The change tendencies of Curie temperature of the $R$Co$_5$ compounds are related to those of two kinds of Co atoms as shown in Fig. 2, for the heavy rare earth element (HRE) -based $R$Co$_5$ are ordered ferrimagnetically. In other words, the 3d magnetic electrons $m^{3\text{d}}$ of LRE in L$R$ECo$_5$ and YCo$_5$ compounds exhibit parallel align-

ment to those of Co while antiparallel in H*R*ECo$_5$ compounds. The direction of the arranged magnetic electrons in Co atoms is defined as being positive, and that in *R* atoms is positive in L*R*ECo$_5$ compounds and it is negative in H*R*ECo$_5$ compounds. For the H*R*ECo$_5$ compounds, the 4f electrons contribute to the moment, the molecular moment equals the sum of 3d and 4f moments, which are negative in the calculated results as presented in Eq. (7). It is nicely consistent with the observed result as shown in the inset of Fig. 1. Figure 2 shows the relationships between $T_c^{cal}$ and $m_{Co^I}^{3d}$ as well as $m_{Co^{II}}^{3d}$, where it can be seen that the change tendency of $T_c^{cal}$–*R* curve seems to be similar to that of $m_{Co^{II}}^{3d}$–*R* curve. It implies that the exchange coupling between Co$^I$ and *R* affects the Curie temperature of *R*Co$_5$. For Co atoms, the moment of Co$^I$ is more than that of Co$^{II}$ atom. In general, Curie temperatures of *R*Co$_5$ are proportional to the average moments per bond number, which reveals the anisotropies of the magnetic exchanging interactions along various bonds. Except for the contribution of 3d–3d or 3d–4f interaction to the ferromagnetic order, the lattice electrons also have an influence on the Curie temperature. As for SmCo$_5$, the large error between the calculated and observed results for Curie temperature might be caused by the electronic transformations from lattice electrons $n_l$ into 3d magnetic electrons $m_{Co^I}^{3d}$ at 3*g* site (see Fig. 3(c)).

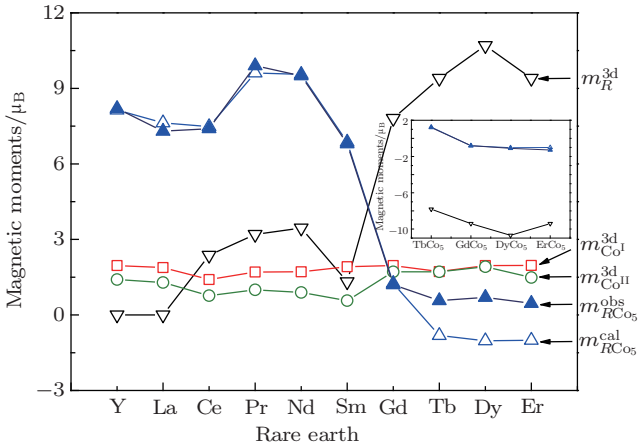



**Fig. 1.** (color online) Calculated results of magnetic moments of *R*-, 2*c*- and 3*g*-sited Co in *R*Co$_5$ compounds. The insert gives the antiferromagnetic interaction between *R* and Co in *R*Co$_5$ compounds when *R* = heavy rare earth.

**Table 2.** Calculation results of magnetic properties. In this table, $n_\alpha$ (max) denotes the maximum number in the covalent electron pairs $n_\alpha$ ($\alpha = A, B, \ldots N$), and the symbol "–" refers to the negative moment originating from the heavy rare earths since their moment arrangements are anti parallel to the direction of 3d moment of Co.

| *R*Co$_5$ | YCo$_5$ | LaCo$_5$ | CeCo$_5$ | PrCo$_5$ | NdCo$_5$ | SmCo$_5$ | GdCo$_5$ | TbCo$_5$ | DyCo$_5$ | ErCo$_5$ |
|---|---|---|---|---|---|---|---|---|---|---|
| $n_\alpha$ (max) | 0.7087 | 0.6853 | 0.5693 | 0.6096 | 0.6251 | 0.6712 | 0.6642 | 0.6378 | 0.6352 | 0.7389 |
| $\lvert\Delta D\rvert$/Å | 0.0074 | 0.0341 | 0.0129 | 0.0250 | 0.0386 | 0.0321 | 0.0297 | 0.0254 | 0.0325 | 0.0221 |
| $(m^{3d}/R)/\mu_B$ | 0 | 0 | 2.37 | 3.2 | 3.45 | 1.32 | –7.81 | –9.4 | –10.7 | –9.4 |
| $(m^{3d}/Co^I)/\mu_B$ | 1.9628 | 1.8837 | 1.4047 | 1.9675 | 1.7120 | 1.9157 | 1.9628 | 1.7241 | 1.9628 | 1.9675 |
| $(m^{3d}/Co^{II})/\mu_B$ | 1.4047 | 1.2876 | 0.7421 | 0.9457 | 0.8936 | 0.5707 | 1.7120 | 1.7120 | 1.9157 | 1.4872 |
| $\overline{m_{Co_5}}/\mu_B$ | 8.1398 | 7.6303 | 7.4058 | 9.9716 | 9.5547 | 6.8634 | 1.2516 | –0.8158 | –1.0273 | –1.0034 |
| $m_{Co_5}/\mu_B$ | 8.2 | 7.3 | 7.4 | 10.0 | 9.5 | 6.8 | 1.2 | 0.8 | 1.1 | 1.28 |
| $\lvert\Delta m/m_{Co_5}\rvert$/% | 0.73 | 4.52 | 0.08 | 0.28 | 0.58 | 0.93 | 4.30 | 1.98 | 6.61 | 21.61 |
| $\overline{T_c}$/K | 881.15 | 854.14 | 717.96 | 937.38 | 927.40 | 769.13 | 1007.08 | 942.93 | 969.82 | 930.61 |
| $T_c$/K | 977 | 840 | 737 | 912 | 910 | 1020 | 1008 | 980 | 966 | 986 |
| $\lvert\Delta T_c/T_c\rvert$/% | 9.81 | 1.68 | 2.58 | 2.78 | 1.91 | 24.57 | 0.09 | 3.78 | 0.40 | 5.62 |

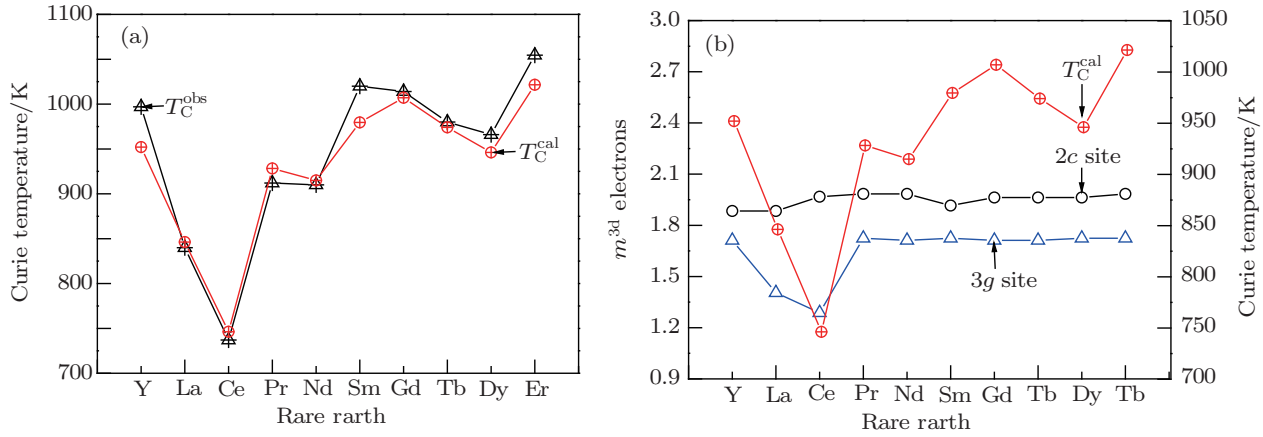



**Fig. 2.** (color online) (a) Observed and calculated Curie temperatures of *R*Co$_5$ and (3d) electron numbers of Co atoms at 2*c* and 3*g* sites.

### 4.3. Analysis of correlation between electronic structure and magnetic property

The calculated valence electronic structures are given in Table 3, and the corresponding electronic transformations are shown in Fig. 3. According to the electron function in electronic binding, the electrons are classified as four categories by EET, which are magnetic electrons, dump pair electrons, lattice electrons, and covalence electrons, denoted by $m^{3d}$, $n_Y$, $n_l$, and $n_c$ respectively. The so-called dump pair electrons represent either a bonding or an anti-bonding electron with their resulting bonding power mutually canceled by each other. The lattice electron, $n_l$ is empirically introduced as a physical quantity, which comes from s electrons. According to the modern quantum theory, the s electrons might reach an energy level above the Fermi energy if the s energy bandgap is wide. In this case, the electrons can hover in lattice space, therefore the electron is so-called lattice electron. Here, two of the four categories of electrons we are talking about, $n_l$ and $n_c$, take part in the formation of an atomic bond by electronic transformation. The $n_T$ equals the sum of $n_l$ and $n_c$.

**Table 3.** Analyses of valence electronic structures of $R$Co$_5$. In this table, $n_c$, $n_l$, $m^{3d}$, and $n_T$ denote the numbers of the covalent electrons, the lattice electrons, the magnetic electrons, and the total number of the electrons, respectively; $\sigma$ is the number of quantum states. The rare earth element has a piece of the hybridization table, which possesses 10 kinds of quantum states. Element Co has 8 pieces of the hybridization table ($A_1$, $A_2$, B, $C_1$, $C_2$, D, $E_1$, $E_2$), and each of them records 18 kinds of quantum states.

| $R$Co$_5$ | | YCo$_5$ | LaCo$_5$ | CeCo$_5$ | PrCo$_5$ | NdCo$_5$ | SmCo$_5$ | GdCo$_5$ | TbCo$_5$ | DyCo$_5$ | ErCo$_5$ |
|---|---|---|---|---|---|---|---|---|---|---|---|
| $\sigma$ | $R$ | 3 | 1 | 1 | 3 | 1 | 1 | 1 | 1 | 3 | 3 |
| | Co$^{I}$ | $E_1$9 | B11 | $E_1$12 | D14 | $A_1$11 | $E_1$10 | $E_1$9 | B12 | $E_1$9 | D14 |
| | Co$^{II}$ | $E_1$12 | B14 | $A_2$10 | $E_2$7 | B15 | $A_2$11 | $A_1$11 | $A_1$11 | $E_1$10 | $E_1$11 |
| $C_h$ | Co$^{I}$ | 0.6543 | 0.6279 | 0.4682 | 0.4873 | 0.5707 | 0.6387 | 0.6543 | 0.5747 | 0.6543 | 0.4837 |
| | Co$^{II}$ | 0.4682 | 0.4292 | 0.7421 | 0.9456 | 0.2979 | 0.5707 | 0.5707 | 0.5707 | 0.6387 | 0.4957 |
| $n_c$ | Co$^{I}$ | 5.6914 | 4.7442 | 6.0737 | 0.0652 | 5.1880 | 5.7228 | 5.6914 | 4.8306 | 5.6914 | 6.0652 |
| | Co$^{II}$ | 6.0737 | 5.1416 | 4.7736 | 5.1089 | 5.4042 | 5.1880 | 5.1880 | 5.1880 | 5.7228 | 6.0085 |
| $n_T$ | Co$^{I}$ | 6.3457 | 6 | 6.5318 | 7.0326 | 6.4293 | 6.3614 | 6.3457 | 6 | 6.3457 | 7.0326 |
| | Co$^{II}$ | 6.5318 | 6 | 6.2579 | 6.0544 | 6 | 6.4293 | 6.4293 | 6.4293 | 6.3614 | 6.5043 |
| $n_l$ | Co$^{I}$ | 0.6543 | 1.2558 | 0.4683 | 0.9674 | 1.1413 | 0.6386 | 0.6543 | 1.1494 | 0.6543 | 0.9674 |
| | Co$^{II}$ | 0.4683 | 0.8584 | 1.4843 | 0.9456 | 0.5958 | 1.1413 | 1.1413 | 1.1413 | 0.6386 | 0.4958 |
| $m^{3d}$ | Co$^{I}$ | 1.9628 | 1.8837 | 1.4872 | 1.9674 | 1.7120 | 1.9157 | 1.9628 | 1.7241 | 1.9628 | 1.9674 |
| | Co$^{II}$ | 1.4872 | 1.2876 | 0.7421 | 0.9456 | 0.8937 | 0.5707 | 1.7120 | 1.7120 | 1.9157 | 1.4047 |
| $R(l)$/Å | $R$ | 1.4721 | 1.5174 | 1.5093 | 1.5353 | 1.4932 | 1.5112 | 1.4600 | 1.4530 | 1.4790 | 1.4629 |
| | Co$^{I}$ | 1.1816 | 1.1938 | 1.1692 | 1.1444 | 1.1331 | 1.1806 | 1.1816 | 1.1923 | 1.1816 | 1.1444 |
| | Co$^{II}$ | 1.1692 | 1.1880 | 1.1617 | 1.2020 | 1.1842 | 1.1331 | 1.1331 | 1.1331 | 1.1806 | 1.1710 |

Figures 3(a) and 3(b) show the electronic transformations among s, p, d, $n_Y$, and $m^{3d}$ electrons in Co$^{I}$ and Co$^{II}$ atoms, respectively. For either of Co$^{I}$ or Co$^{II}$, the electronic transformation between p and d electrons happens in the form of equivalent electrons. As for the electronic transformation between the $m^{3d}$ and $n_Y$ electrons, it reveals the correlation between $m^{3d}$ and d electrons. When the $m^{3d}$ meets with the d electrons, with their resulting bonding power mutually canceled by each other and their spins are opposite to each other, the electron transformation between $m^{3d}$ and $n_Y$ occurs. The number variation of $m^{3d}$ depends upon the electrons transforming from the other electrons into the 3d magnetic electrons. The final numbers of $m^{3d}$ electrons in Co$^{I}$ and Co$^{II}$ atoms make their differences of the contributions to molecular moments and Curie temperature. For Co atoms, the moment of Co$^{I}$ is bigger than that of Co$^{II}$, which is due to the decrease of $m^{3d}$ electrons induced by electron transformation between $m^{3d}$ and $n_c$ of Co$^{I}$. Figures 3(c) and 3(d) show the electronic transformations between $n_l$ or $n_c$or $n_T$ and $m^{3d}$ electrons in Co$^{I}$- and Co$^{II}$ atoms, respectively. The exchange coupling interactions between $m^{3d}$ and $n_l$ of Co$^{II}$ in L$R$ECo$_5$ compounds are the strongest, while those of Co$^{I}$- in H$R$Co$_5$ compounds are the strongest. Taking CeCo$_5$ for example, the numbers of $n_l$ in Co$^{I}$- is the least and the numbers of $n_l$ in Co$^{II}$ is the largest, which keep the balance in the final number of $n_l$. The $n_l$ originates from the s orbital electrons, and s mainly derives from the equivalent p and d electrons. For the H$R$ECo$_5$ compounds, the 4f electrons also contribute to moments, the molecular moment equals the sum of 3d and 4f moments. Figures 3(e) and 3(f) show that the electronic numbers of $n_l$ and $n_c$ electrons at Co$^{I}$ and Co$^{II}$ crystal positions change with the rare earth elements. The changes seem to be the same.

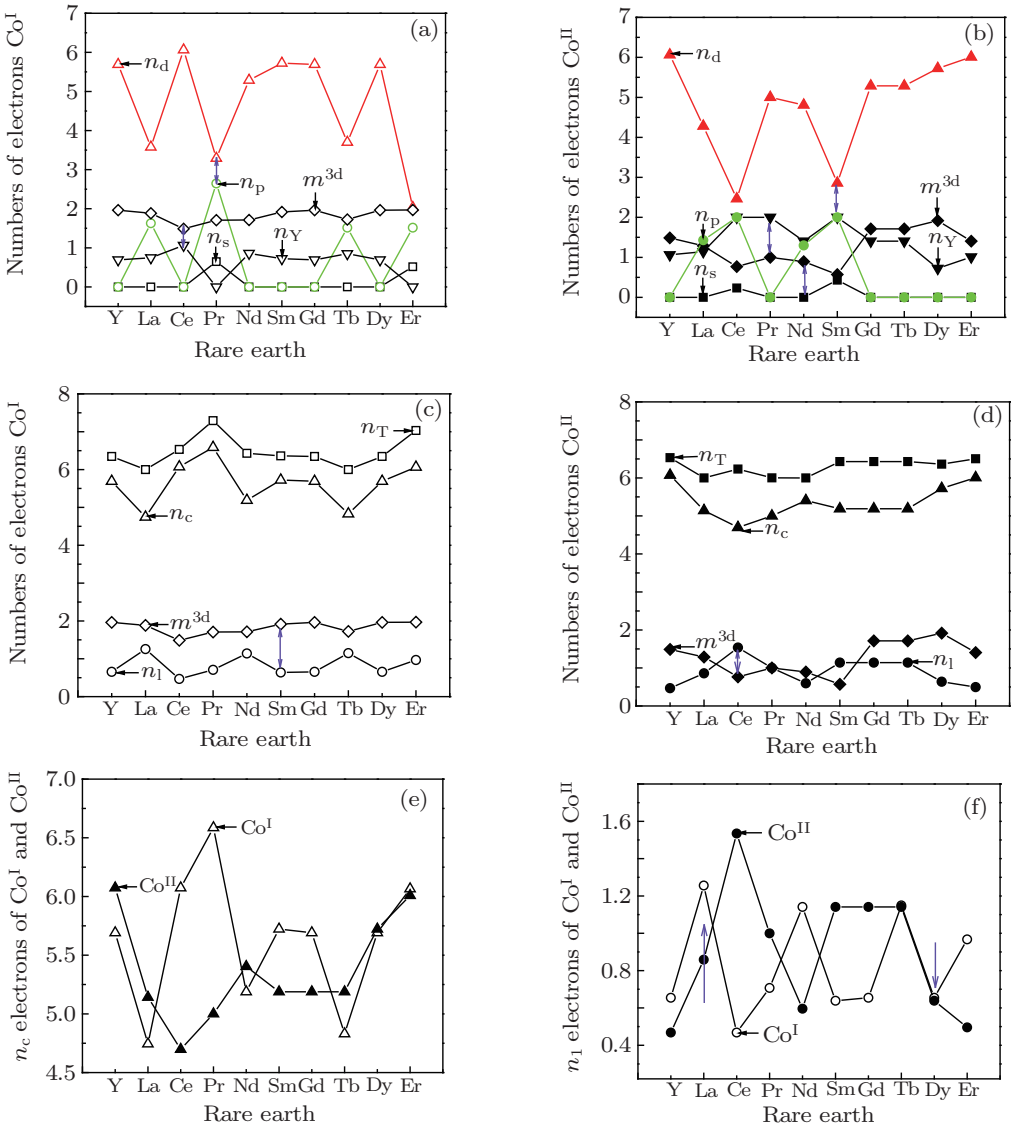



**Fig. 3.** (color online) Electronic transformations among all kinds of electrons. The electronic distributions of Co at 2*c* site (a) and 3*g* site (b); the electron transformations among the covalence, lattice, 3d magnetic electrons are shown for Co at 2*c* site (c) and for Co at 3*g* site (d); the covalence and lattice electrons distributions for $Co^{I}$ and $Co^{II}$ are shown in panels (e) and (f).

## 5. Conclusions and perspectives

The empirical electron theory of solids and molecules (EET), which is based on the Pauling's valance theory, is used to investigate the valence electronic structures and multiple physical properties of solid state materials. The theoretical model is simpler with fewer theoretical parameters than the first principle and the molecular field theory. In this study, the magnetic moments and Curie temperatures of $RCo_5$ ($R$ = rare earth) intermetallics are systematically studied with EET.

The calculated results reveal that the moments of $RCo_5$ intermetallics originate mainly from the 3d electrons of Co atoms and 4f electrons of rare earth, the s electrons also affect the magnetic moments by the hybridization of d and s electrons. The contribution to the moment depends on the sublattices of Co and $R$ atoms, and it is found that the moment of Co atom at 2*c* site is bigger than that at 3*g* site due to the bonding effect between $R$ and Co associated with a electron transformation from 3d electrons into covalence electrons. In the heavy rare-earth-based $RCo_5$ intermetallics, the contribution to the molecular moment originates from 3d and 4f electrons. Curie temperatures of $RCo_5$ are proportional to the average moment along the various bonds, and it indicates the magnetic anisotropy along the various crystal directions. The covalence electrons and lattice electrons also affect the Curie temperature. $RCo_5$ intermetallic compounds show strong relationships between their valence electronic structure and magnetic properties. Except for the 3d–3d or 3d–4f exchange coupling interaction contributing to the ferromagnetic order, the lattice electrons also affect the Curie temperature.

## References

[1] Larson P, Mazin I I and Papaconstantopoulos D A 2003 *Phys. Rev. B* **67** 214405

[2] Malik S K, Arlinghaus F J and Wallace W E 1977 *Phys. Rev. B* **16** 1242

[3] Li Z B, Lan J T, Zhang X F, Liu Y L and Li Y F 2015 *Chin. Phys. B* **24** 087501
[4] Herbst J F and Hector L G 2007 *J. Alloys Compd.* **188** 446
[5] Han X F, Yang F M, Zeng Z, Zheng Q Q, Wang X F, Jin H M and Sun J Z 1997 *Acta Phys. Sin.* (Overseas Edition, i.e., *Chin. Phys.*) **6** 697
[6] Sankar S G, Rao V U S, Segal E, Wallace W E, Frederick W G D and Garrett H J 1975 *Phys. Rev. B* **11** 435
[7] Rao V U S and Greedan J E 1973 *J. Solid State Chem.* **6** 387
[8] Chen T L and Wang Q 2000 *Commun. Theor. Phys.* **34** 6
[9] Zhao T S, Jin H M, Guo G H, Han X F and Chen H 1991 *Phys. Rev. B* **43** 8593
[10] Tadaei I and Hideaki I 2005 *J. Appl. Phys.* **97** 10A313
[11] Hector L G and Herbst J F 2003 *Appl. Phys. Lett.* **82** 1042
[12] Liebs M, Hummler K, Beuerle T, Ubele P and Fahnle M 1995 *J. Magn. Magn. Mater.* **140–144** 851
[13] Miletić G I and Blažina Ž 2007 *J. Solid State Chem.* **180** 604
[14] Miletić G I and Blažina Ž 2009 *J. Magn. Magn. Mater.* **321** 3888
[15] Richter M, Oppeneer P M, Eschrig H and Johansson B 1992 *Phys. Rev. B* **46** 13919
[16] Beloritzky E, Fremy M A, Gavigan J P, Givord D and Li H S 1987 *J. Appl. Phys.* **61** 3971
[17] Hu B P, Li H S, Gavigan J P and Coey J M D 1990 *Phys. Rev. B* **41** 2221
[18] Kokorina E E, Medvedev M V and Nekrasov I A 2010 *International Conference on Magnetic Materials*, October 25–29, 2010, Kolkata, India, p. 75
[19] Yu R H 1978 *Chin. Sci. Bull.* **23** 217 (in Chinese)
[20] Cao Z X 2014 *Chin. Phys. B* **23** 063102
[21] Zhang J F, Zhang M, Zhao Y W, Zhang H Y, Zhao L N and Luo Y H 2015 *Chin. Phys. B* **24** 067101
[22] Fang S S and Qiao H X 2015 *Chin. Phys. B* **24** 083101
[23] Guo Y Q, Yu R H, Zhang R L, Zhang X H and Tao K 1998 *J. Phys. Chem. B* **102** 9
[24] Wu W X, Guo Y Q, Li A H and Li W 2008 *Acta Phys. Sin.* **57** 2486 (in Chinese)
[25] Meng Z H, Guo Y Q, Li J B and Wang Y 2012 *Acta Phys. Sin.* **61** 107101 (in Chinese)
[26] Lin C, Yin G L and Zhao Y Q 2015 *Comp. Mater. Sci.* **101** 168
[27] Shen J, Qian P and Chen N X 2004 *J. Phys. Chem. Solids* **65** 1307
[28] Givord D, Deportes J, Schweizer J and Tasset F 1976 *IEEE. Trans. Magn.* **12** 1000